Journal of Sound and Vibration (2000) **234**(2), 177–189
doi:10.1006/jsvi.1999.2874, available online at http://www.idealibrary.com on IDEAL®

TOPOLOGY OPTIMIZATION OF STRUCTURES UNDER DYNAMIC RESPONSE CONSTRAINTS

J. H. Rong

Aircraft Strength Research Institute, AVIC, PO Box 86, *Xi'an* 710065, *People's Republic of China*

AND

Y. M. Xie, X. Y. Yang and Q. Q. Liang

Faculty of Engineering and Science, Victoria University of Technology, PO Box 14428, *Melbourne City MC, VIC* 8001, *Australia*

(*Received* 26 *June* 1999, *and in final form* 29 *October* 1999)

In recent years, the Evolutionary Structural Optimization (ESO) method has been developed into an effective tool for engineering design. However, no attempts have been made to incorporate random dynamic response constraints. The optimum design of structures with dynamic response constraints is of great importance, particularly in the aeronautical and automotive industries. This paper considers the extension and modification of the ESO method to control the structural random dynamic responses. The random dynamic theory is applied to build an expression of random dynamic response constraints considering engineering requirements. Based on the modal truncation method of eigenderivatives and some approximate process, a set of formulations for sensitivity numbers of mean square random dynamic responses is derived. The algorithm is implemented in optimization software. Several examples are provided to demonstrate the validity and effectiveness of the proposed method.

1. INTRODUCTION

Evolutionary Structural Optimization (ESO) has been developed based on the simple concept that by systematically removing the unwanted material, the residual shape of the structural evolves towards an optimum [1–3]. It has the advantages of clear concept and easy mathematical operation compared to conventional analytical and numerical optimization methods. Extensive research has been done on the ESO method for various types of structures and the optimality constraints can be stress based, stiffness/displacement based, frequency and bulking load based [3]. Its wide coverage demonstrates that it is capable of solving all kinds of structural optimization problems in practical engineering.

However, no attempts have been made to incorporate random dynamic response constraints. Aircraft and aerospace vehicles are subjected to diverse sources of random dynamic excitation during their service life. Such excitations include: (a) the ground loads induced during taxi, takeoff and landing of an aircraft, or during the transportation of a launch vehicle to the launch pad; (b) the gust excitation caused by atmospheric turbulence; (c) the aerodynamic excitation due to boundary layer turbulence and fluctuating wake forces; and (d) the excitation due to jet and rocket noise. Therefore, the design of aircraft

0022-460X/00/270177 + 13 $35.00/0

structures must deal with the effect of structural dynamic responses on the aircraft structure. Studies of dynamic response optimization have been mainly restricted to changing the size of beams or the thickness of plates [4–7]. A bibliography on this topic can be found in a survey by Grandhi [8]. More recent attempts on the simultaneous shape and topology optimization of different design objectives including frequency/dynamic response have achieved some success. The most notable advance is the homogenization method [9, 10], the density function method [11, 12] and the continuum formulations [13, 14]. Also, repeated frequency as encountered in dynamic problems especially in the above-mentioned aircraft design has been investigated extensively [14–18].

This paper addresses the optimal topology design for structures with random dynamic response constraints using he ESO method. An expression of mean square random dynamic response constraints is first established based on the random vibration theory and considering practical engineering requirements. Using the modal truncation method of eigenderivatives, the sensitivity number of frequencies and mode shapes is formulated, and then the sensitivity number of mean square random dynamic responses is derived. The structural modification is based on the sensitivity number and the ESO procedure is performed in such a way that the element with the smallest sensitivity number is removed. The proposed procedure is tested on four examples in corporation with the finite element analysis.

2. DESCRIPTION OF RANDOM VIBRATION

It is often required in the dynamic design that the mean square responses of some nodes in a structure under the action of random excitations are within some prescribed limits. This section is to formulate the expression of such a requirement based on the modal analysis theory [6, 19].

The finite element equation for a structural dynamic problem can be written in the form

$$[M]\{\ddot{Y}\} + [C]\{\dot{Y}\} + [K]\{Y\} = \{f(t)\}, \tag{1}$$

where $[M]$, $[C]$ and $[K]$ are the $N \times N$ mass, damping, and stiffness matrices of the structure respectively. N is the number of degree of freedom. $\{f(t)\}$ is the random excitation force vector, and $\{Y\}$, $\{\dot{Y}\}$ and $\{\ddot{Y}\}$ are the displacement, velocity and acceleration vectors.

Assume that the system of equation (1) is of proportional damping; using the mode superposition method, equation (1) can be uncoupled as

$$\ddot{q}_i + 2\omega_i\zeta_i\dot{q}_i + \omega_i^2 q_i = p_i \quad (i = 1, 2, 3, \ldots, n), \tag{2a}$$

where q_i is the modal co-ordinates defined by

$$\{Y\} = [\{\varphi_1\}, \{\varphi_2\}, \ldots, \{\varphi_n\}] \begin{Bmatrix} q_1 \\ q_2 \\ \cdots \\ q_n \end{Bmatrix} = [\Phi]\{q\}. \tag{2b}$$

In the above equations, ω_i and $\{\varphi_i\}$ are the ith circular frequency and mode shape normalized with respect to the mass matrix. ζ_i is the mode damping ratio of ith mode. p_i represents the ith element of $[\Phi]^{\mathrm{T}}\{f(t)\}$ and is called the ith generalized excitation. n is the number of truncated modes.

We consider here that the structure is under white-noise excitation. This can be an idea simulation of practical wide band random excitation. Assume that the excitation force vector is of zero mean values and auto-power spectral $[D]$, i.e.,

$$E[\{f(t)\}] = \{0\}, \qquad E[\{f(t)\}\{f(t+\tau)\}^{\mathrm{T}}] = 2\pi[D]\delta(\tau). \tag{3}$$

Therefore, it follows that

$$E[\{p(t)\}] = \{0\}, \qquad E[\{p(t)\}\{p(t+\tau)\}^{\mathrm{T}}] = 2\pi[\Phi]^{\mathrm{T}}[D][\Phi]\delta(\tau). \tag{4}$$

The statistics characteristics of dynamic response can be derived from the conditions given by equations (1)–(4). Detailed derivation can be found in reference [6] and only main conclusions are provided here for the sake of brevity. Light damping is assumed in derivation, i.e., $\zeta_i < 1$. Define

$$[\Phi]^{\mathrm{T}}[D][\Phi] = [d_{rs}], \tag{5}$$

the correlation matrix of mode response is

$$[R_{qrqs}(\tau)] = E[\{q_r(t)\}\{q_s(t+\tau)\}], \tag{6}$$

where the element when $\tau = 0$ is given as

$$R_{q_r q_s}(0) = \frac{\pi d_{rs} a_{rs} r_{rs}}{\eta_r \eta_s \omega_r \omega_s} \equiv C_{rs}, \quad r \neq s, \tag{7a}$$

where

$$a_{rs} = \zeta_r \omega_r + \zeta_s \omega_s, \qquad r_{rs} = Q_{rs} - g_{rs}, \qquad g_{rs} = (a_{rs}^2 + b_{rs}^2)^{-1}, \tag{7b}$$

$$Q_{rs} = (a_{rs}^2 + e_{rs}^2)^{-1}, \qquad b_{rs} = \eta_r \omega_r + \eta_s \omega_s, \qquad e_{rs} = \eta_r \omega_r - \eta_s \omega_s \tag{7c}$$

and the diagonal elements can be found in a simple form as

$$R_r = \left(\frac{\pi d_r}{2\zeta_r \omega_r^3}\right), \tag{7d}$$

which represents the autocorrelation function of the mode response.

Therefore, the covariance matrix of response Y is

$$[\bar{B}_{Y_r Y_s}] = [R_{Y_r Y_s}(0)] = [\Phi][R_{q_r q_s}(0)][\Phi]^{\mathrm{T}}. \tag{8}$$

From equations (7a)–(8), the mean square response of the ith degree of freedom Y_i can be expressed as

$$\sigma_{Y_i}^2 = \sum_{r=1}^{n} \sum_{s=1}^{n} \varphi_{ir} C_{rs} \varphi_{is} \quad (i = 1, 2, \ldots, N). \tag{9}$$

As a special case, if the generalized excitation on all degrees of freedom of the system are not correlated with each other, i.e. $[\Phi]^{\mathrm{T}}[D][\Phi] = diag(d_i)$, equation (9) is reduced to

$$\sigma_{Y_i}^2 = \sum_{r=1}^{n} (\varphi_{ir})^2 \frac{\pi d_{rr}}{2\zeta_r \omega_r^3} \quad (i = 1, 2, \ldots, N). \tag{10}$$

3. PROBLEM STATEMENTS

3.1. FORMULATION OF OPTIMIZATION PROBLEM

In aircraft design, a general goal is to minimize the structural weight while satisfying the requirements of structural working characteristics. Therefore, the topology optimization problem of a continuum structure under dynamics response constraints can be stated as follows:

Minimize

$$W = \sum_{e=1}^{m} w_e \tag{11a}$$

Subject to

$$\sigma_{\dot{Y}_i}^2 \leqslant (\sigma_{\dot{Y}_i}^2)^u \quad (i = 1, 2, \ldots, p), \tag{11b}$$

where W is the total weight of the structure and w_e is the weight of the eth element. $(\sigma_{\dot{Y}_i}^2)^u$ is the prescribed limit of $\sigma_{\dot{Y}_i}^2$ and p is the total number of dynamics response constraints.

3.2. SENSITIVITY NUMBER FOR DYNAMIC RESPONSES

Sensitivity analysis is used to identify the best locations for structural modifications to reach a desired optimal design. For the formulation posed in equations (11a)–(11b), sensitivity analysis is to determine the effect of an element removal on the mean square response $\sigma_{\dot{Y}_i}^2$.

To perform the above sensitivity analysis involves the derivatives of eigenvalues and eigenderivatives. At present, there are a number of efficient methods for calculating eigenvector derivatives, such as the finite-difference method, the modal truncation method [20], the modal method [21, 22], Nelson's method [23] and an improved modal method [24, 25]. Haftka and Adelman [26] and Baldwin and Hutton [27] surveyed developments in this area. The eigenvector analysis in the paper is based on the modal truncation method.

Suppose that the jth element is removed from the current structure. The change of the global stiffness and mass matrices due to such a removal is

$$[\Delta K] = -[K^j], [\Delta M] = -[M^j], \tag{12}$$

where $[K^j]$ and $[M^j]$ are the element stiffness and mass matrices.

The eigenvalue sensitivity and eigenvector sensitivity are

$$\Delta(\omega_i^2) = \{\varphi_i\}^{\mathrm{T}}([\Delta K] - \omega_i^2[\Delta M])\{\varphi_i\}, \tag{13a}$$

$$\{\Delta\varphi_i\} = \sum_{k=1}^{n} \beta_{ik}\{\varphi_k\}, \tag{13b}$$

where

$$\beta_{ii} = -\tfrac{1}{2}\{\varphi_i\}^{\mathrm{T}}[\Delta M]\{\varphi_i\} \tag{13c}$$

and

$$\beta_{ik} = \frac{\{\varphi_k\}^{\mathrm{T}}([K]_j - \omega_i^2[M]_j)\{\varphi_i\}}{\omega_i^2 - \omega_k^2}, \quad k \neq i. \tag{13d}$$

In deriving the sensitivity of mean square response, it is assumed that the white-noise excitations on all degrees of freedom of the system are not correlated with each other, i.e. $[D] = diag(D_i)$. Therefore, it follows that $[\Phi]^{\mathrm{T}}[D][\Phi] = [d_{rs}]$ in equation (5) is expressed as

$$d_{rs} = \sum_{i=1}^{N} \varphi_{ir}\varphi_{is}D_i. \tag{14}$$

Assume that the modal damping ration $\zeta_r (r = 1, 2, \ldots, n)$ does not change significantly in between cycles. From equations (7a), (9) and (10), the sensitivity of mean square response is as follows:

Case 1 corresponding to equation (9):

$$\alpha_{ij} = \Delta\sigma_{Y_i}^2 = \sum_{r=1}^{n}\sum_{s=1}^{n}(\Delta\varphi_{ir}C_{rs}\varphi_{is} + \varphi_{ir}\Delta C_{rs}\varphi_{is} + \varphi_{ir}C_{rs}\Delta\varphi_{is}) \quad (i = 1, 2, \ldots, p;\ j = 1, 2, \ldots, m), \tag{15a}$$

in which

$$\Delta C_{rs} = -\frac{\pi d_{rs}a_{rs}r_{rs}}{\eta_r\eta_s\omega_r^2\omega_s^2}\left(\frac{\Delta(\omega_r^2)\omega_s}{2\omega_r} + \frac{\Delta(\omega_s^2)\omega_r}{2\omega_s}\right) + \frac{\pi\Delta d_{rs}a_{rs}r_{rs}}{\eta_r\eta_s\omega_r\omega_s} + \frac{\pi d_{rs}\Delta a_{rs}r_{rs}}{\eta_r\eta_s\omega_r\omega_s} + \frac{\pi d_{rs}a_{rs}\Delta r_{rs}}{\eta_r\eta_s\omega_r\omega_s} \quad (r = 1, 2, \ldots, n;\ s = 1, 2, \ldots, n), \tag{15b}$$

$$\begin{aligned}\Delta d_{rs} &= \sum_{i=l}^{N}(\varphi_{ir}\Delta\varphi_{is} + \varphi_{is}\Delta\varphi_{ir})D_l \\ &= \sum_{k=l}^{n}\left(\beta_{sk}\sum_{i=l}^{N}\varphi_{ir}\varphi_{lk}D_l + \beta_{rk}\sum_{l=l}^{N}\varphi_{is}\varphi_{ik}D_l\right) \\ &= \sum_{k=l}^{n}(\beta_{sk}d_{rk} + \beta_{rk}d_{sk}) \quad (r = 1, 2, \ldots, n;\ s = 1, 2, \ldots, n),\end{aligned} \tag{15c}$$

$$\Delta a_{rs} = \frac{\zeta_r}{2\omega_r}\Delta(\omega_r^2) + \frac{\zeta_s}{2\omega_s}\Delta(\omega_s^2) \quad (r = 1, 2, \ldots, n;\ s = 1, 2, \ldots, n), \tag{15d}$$

$$\Delta r_{rs} = -Q_{rs}^2(2a_{rs}\Delta a_{rs} + 2e_{rs}\Delta e_{rs}) + g_{rs}^2(2a_{rs}\Delta a_{rs} + 2b_{rs}\Delta b_{rs}), \tag{15e}$$

$$\Delta b_{rs} = \frac{\eta_r}{2\omega_r}\Delta(\omega_r^2) + \frac{\eta_s}{2\omega_s}\Delta(\omega_s^2), \tag{15f}$$

$$\Delta e_{rs} = \frac{\eta_r}{2\omega_r}\Delta(\omega_r^2) - \frac{\eta_s}{2\omega_s}\Delta(\omega_s^2), \tag{15g}$$

$$a_{rs} = \zeta_r\omega_r + \zeta_s\omega_s, \qquad r_{rs} = Q_{rs} - g_{rs}, \qquad g_{rs} = (a_{rs}^r + b_{rs}^2)^{-1}, \tag{15h}$$

$$Q_{rs} = (a_{rs}^2 + e_{rs}^2)^{-1}, \qquad b_{rs} = \eta_r\omega_r + \eta_s\omega_s, \qquad e_{rs} = \eta_r\omega_r - \eta_s\omega_s. \tag{15i}$$

Case 2 corresponding to equation (10):

$$\alpha_{ij} = \Delta\sigma_{Y_i}^2 = \sum_{r=1}^{n}\varphi_{ir}\frac{\pi d_{rr}}{\zeta_r\omega_r^3}\Delta\varphi_{ir} - \sum_{r=l}^{n}\frac{3\pi d_{rr}(\varphi_{ir})^2}{4\zeta_r\omega_r^5}\Delta\omega_r^2, + \sum_{r}^{n}\frac{\pi(\varphi_{ir})^2}{\zeta_r\omega_r^3}\left(\sum_{i=l}^{N}\varphi_{ir}\Delta\varphi_{ir}D_l\right) \quad (i = 1, 2, \ldots, p;\ j = 1, 2, \ldots, m), \tag{16a}$$

$$d_{rr} = \sum_{l=l}^{N}(\varphi_{ir})^2D_l \quad (r = 1, 2, \ldots, n). \tag{16b}$$

3.3. OPTIMALITY CRITERIA

The Lagrangian function for the multiple constraint problem of equation (11a)–(11b) is given as

$$L = W - \sum_{i=1}^{p} \lambda_i (\sigma_{Y_i}^2 - (\sigma_{Y_i}^2)^u), \tag{17}$$

where λ_i is the Lagrange multiplier for the ith constraint. Using an approach similar to that in reference [28], the optimality criterion is

$$\gamma_j = \sum_{i=1}^{p} \frac{\lambda_i \alpha_{ij}}{w_i} = \sum_{i=1}^{p} \lambda_i \frac{s_{ij}}{\rho_j} = 1 \quad (j = 1, 2, \ldots, m), \tag{18}$$

where ρ_j is the mass density, v_j is the volume with $w_j = \rho_j v_j$ and $s_{ij} = \alpha_{ij}/v_j$. Therefore, the sensitivity number for element removal for multiple dynamic response constraint problem is defined as

$$\gamma_j = \sum_{i=1}^{p} \lambda_i \frac{\alpha_{ij}}{w_i} \quad (j = 1, 2, \ldots, m), \tag{19}$$

which implies that the sensitivity number for multiple dynamic response constraints is the weighted sum of the sensitivity numbers corresponding to each constraint.

In topology optimization of static displacements, different schemes have been suggested to determine the Lagrange multipliers [28, 29]. The way adopted here is the ratio formulae given as

$$\lambda_i = \left(\frac{\sigma_{Y_i}^2}{\varphi (\sigma_{Y_i}^2)^u} \right)^{1/b} \quad (i = 1, 2, \ldots, p), \tag{20}$$

where b is a step control parameter and $\varphi = \max_{i=1,p}(\sigma_{Y_i}^2/(\sigma_{Y_i}^2)^u)$ is a scaling factor, which is introduced to keep constraints active.

3.4. EVOLUTIONARY OPTIMIZATION PROCEDURE

The evolutionary procedure for topology optimization of a structure subject to random dynamic response constraints is summarized as follows:

Step 1: Define a ground structure (initial FEA model) for the structure.

Step 2: Analyze the structure for the given random load cases.

Step 3: Calculate the element sensitivity number γ_j by equation (19).

Step 4: Remove a number of elements that have the lowest sensitivity numbers.

Step 5: Repeat Steps 2–4 until one of the constrained random dynamic response reaches its prescribed limit or the sensitivity numbers become uniform.

The number of elements to be removed at each iteration is prescribed by the element removal ratio (*ERR*). It is defined by the ratio of the number of removed elements to the total number of elements of the initial or the current FEA model. The values up to 10% for *ERR* have been used by Chu *et al.* [28] for topology optimization with static displacement constraints. The presence and absence of an element is described by non-zero and zero. An element removed at the current structure is tagged 0 so that it will be ignored in the subsequent finite element analysis. For finite analysis using four-node elements, it is noted that in some iteration an element may be connected to the other elements only at one node. As such an element does not have in-plane rotation stiffness corresponding to drilling freedom and it can have free in-plane rotation, the stiffness matrix will become singular.

A simple measure to overcome singularity of stiffness matrix is to introduce a check procedure on the completion of element modification and remove the singular elements accordingly.

Further, it is noted the square root of objective function (σ_Y) is proportional to the reciprocal of the design variables (plate thickness t) or its nth order, i.e., $\sigma_Y = c(1/t)^n$ where c is a constant. n is 1 for the plane stress case and 3 for plate bending case. A single scale procedure is applicable. In doing so, the topology of a design remains unchanged but the thickness is scaled so that the response of the concerned node is equal to the prescribed limit $(\sigma_Y)^u$. The weight of a design after scaling is called the objective weight. The ratio between the objective weight of the current structure and that of the initial design is called weight ratio. It is clear from this definition that the weight ratio of the initial design is 1 and a topology of smaller weight ratio represents a better optimum solution.

4. EXAMPLES

In the following examples, the formulation of mean square dynamic responses and their sensitivity numbers are calculated by using equations (7a)–(7d), (9) and (15a)–(15i).

4.1. A BENDING PLATE STRUCTURE UNDER SINGLE LOAD AND ONE-POINT DYNAMIC RESPONSE CONSTRAINT

Figure 1 shows an initial structural model and its loading conditions. The prescribed limit of mean square dynamic response in the vertical direction of point A is 0·011 m^2. The initial mean square dynamic response at the same point is 0·0020 m^2 under the action of autopower spectral $D_A = 1{\cdot}0\ N^2/Hz$. The Young's modules $E = 207$ GPa, the Poisson ratio $v = 0{\cdot}3$, thickness $t = 0{\cdot}005$ m and mass density $\rho = 2700\ kg/m^3$ are assumed. The design domain is divided into a mesh of 48×16, namely 768 four-node bending plate finite elements and removal ratio 1% is used at each step.

Two cases are investigated. The number of truncated modes in the first case is 14 and the number in the second case is 19. The evolutionary histories of the mean square dynamic responses of the two cases are illustrated in Figure 2. It is seen that by slowly removing elements with the smallest sensitivity number, the response is gradually increased. The remaining elements represent the optimal topology as shown in Figures 3 and 4. It is seen that results obtained by using different truncated mode numbers agree well with each other. Also, the optimum topology in Figure 4(b) has a weight ratio of 0·4219, representing a significant topology improvement over the initial design.

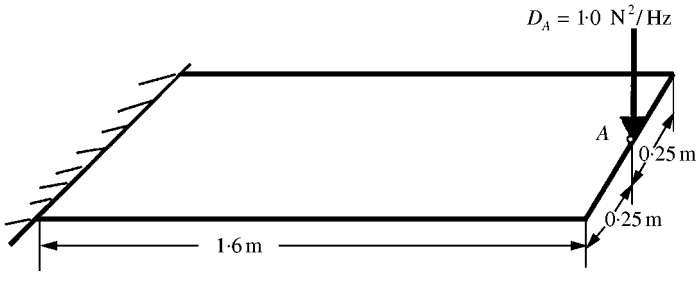

Figure 1. The structural model and loading case of a bending plate.

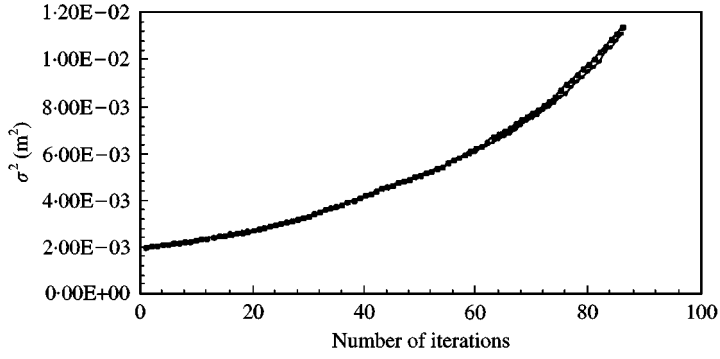

Figure 2. Evolutionary histories of mean square dynamic responses at point A by using two different mode numbers: (——) results obtained by using 14 modes; (—▲—) result obtained by using 19 modes.

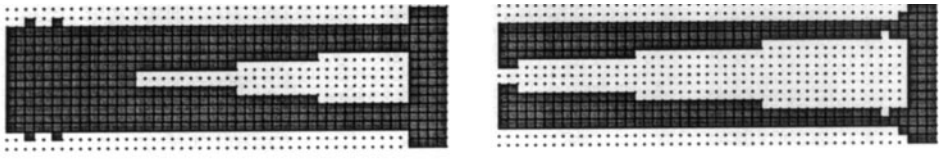

Figure 3. Optimization of the bending plate model by using 14 modes: (a) topology at iteration 45, weight ratio = 0·6276. $\sigma_A^2 = 0{\cdot}004741\ \mathrm{m}^2$; (b) optimum topology weight ratio = 0·4219. $\sigma_A^2 = 0{\cdot}01080\ \mathrm{m}^2$.

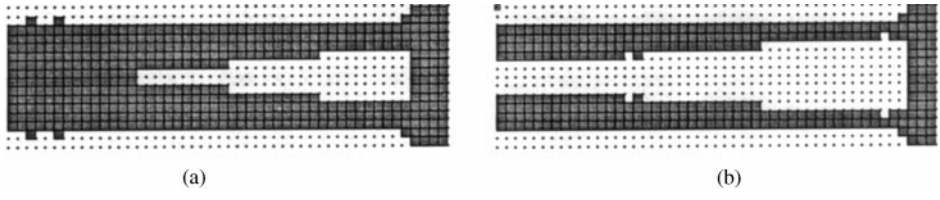

Figure 4. Optimization of the bending plate model by using 19 modes: (a) topology at iteration 45, weight ratio = 0·6276. $\sigma_A^2 = 0{\cdot}004751\ \mathrm{m}^2$; (b) optimum topology weight ratio = 0·4219. $\sigma_A^2 = 0{\cdot}01087\ \mathrm{m}^2$.

4.2. BENDING PLATE WITH MULTIPLE RESPONSE REQUIREMENTS

Figure 5 shows the initial structural model and its loading conditions. It has the same geometrical and material properties and finite element mesh as example 1. The autopower spectral D_A, D_D and D_E of dynamic loads imposed at points A, D and E, are 1·0, 2·0 and 2·0 N^2/Hz respectively. The corresponding limits of mean square dynamic responses applied downward are 0·05, 0·018 and 0·018 m^2 respectively. Element removal ratio $ERR = 1\%$ is used. The evolutionary histories of the mean square dynamic responses at the three points are illustrated in Figure 6. Figure 7 gives the topologies with different weight ratios.

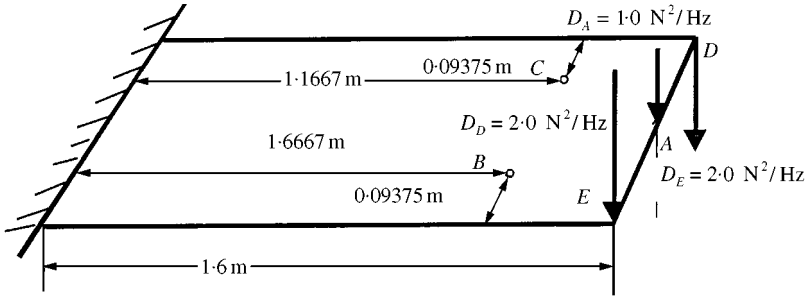

Figure 5. The initial structure model and loading case of a bending plate.

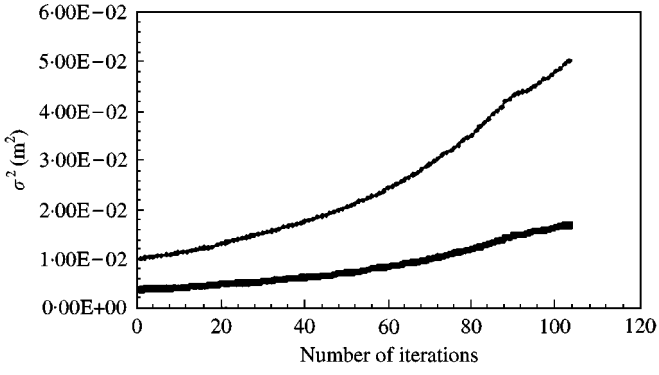

Figure 6. Evolutionary history of mean square dynamic responses at points *A*, *B* and *C*: (——) mean square response at point *A*; (—▲—) mean square response at node *C*; (—■—) mean square response at node *B*.

4.3. A PLATE UNDER PLANE STRESS CONDITION

Another example is a plate under the plane-stress condition fixed at the left side, as shown in Figure 8. It has the same material properties as example 1. The initial design is divided into a mesh of 48×30, namely 1440 four-node plane-stress finite elements. The thickness is 0·001 m and $ERR = 0{\cdot}8\%$ is used. The limit of the mean square dynamic response at point *A* is $0{\cdot}05\ \mathrm{mm}^2$ under the applied load of autopower spectral $D_A = 1{\cdot}0\ \mathrm{N}^2/\mathrm{Hz}$. Figure 9 shows the evolutionary history of the mean square dynamic response at point *A*, and Figure 10 give the topologies. The optimum topology is shown in Figure 10(d), with a mean square response $0{\cdot}04971\ \mathrm{mm}^2$ and a weight ratio 0·4556.

4.4. A PLATE STRUCTURE WITH A NON-SYMMETRIC APPLIED LOAD

The final example is a plate with a non-symmetric load. Figure 11 shows the structural model and its loading conditions. It has the same geometrical, material properties and finite element mesh case as example 3. The limit of mean square dynamic responses in the vertical direction of point *A* is $0{\cdot}05\ \mathrm{mm}^2$. The evolutionary history is shown in Figure 12. The optimum topology is given in Figure 13 with a mean square dynamic response equal to $0{\cdot}04911\ \mathrm{mm}^2$.

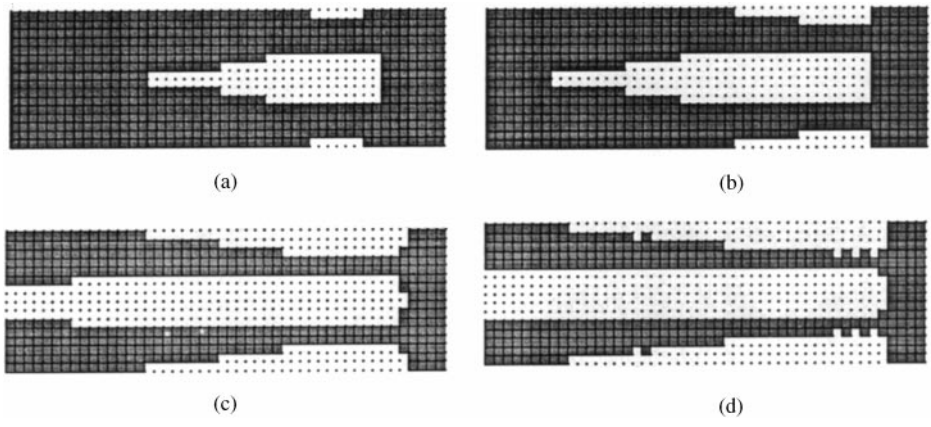

Figure 7. Optimization of the bending plate model considering multiple dynamic response requirements: (a) topology at iteration 20, weight ratio = 0·8438. $\sigma_A^2 = 0{\cdot}01289$, $\sigma_B^2 = 0{\cdot}004767$ and $\sigma_C^2 = 0{\cdot}004767\ m^2$; (b) topology at iteration 40, weight ratio = 0·7292. $\sigma_A^2 = 0{\cdot}01764$, $\sigma_B^2 = 0{\cdot}006187$ and $\sigma_C^2 = 0{\cdot}006187\ m^2$; (c) topology at iteration 80, weight ratio = 0·5208. $\sigma_A^2 = 0{\cdot}03569$, $\sigma_B^2 = 0{\cdot}01194$ and $\sigma_C^2 = 0{\cdot}01194\ m^2$; (d) optimum topology, weight ratio = 0·4453. $\sigma_A^2 = 0{\cdot}04958$, $\sigma_B^2 = 0{\cdot}01649$ and $\sigma_C^2 = 0{\cdot}01649\ m^2$.

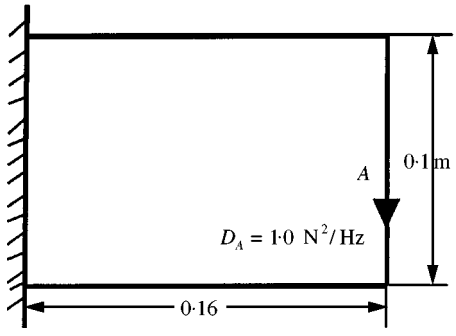

Figure 8. The initial structure model and loading case of plane-stress plate.

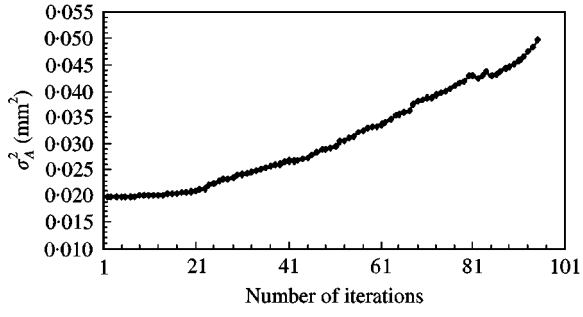

Figure 9. Evolutionary history of the mean square dynamic response at point *A*.

It is noted that the accuracy of sensitivity analysis using the modal truncation method may depend on the numbers of involved modes. In the first example, it is seen that the number of truncated modes does not have distinct effect on the optimum solution. However, this point can be problem dependent and is currently under investigation. One

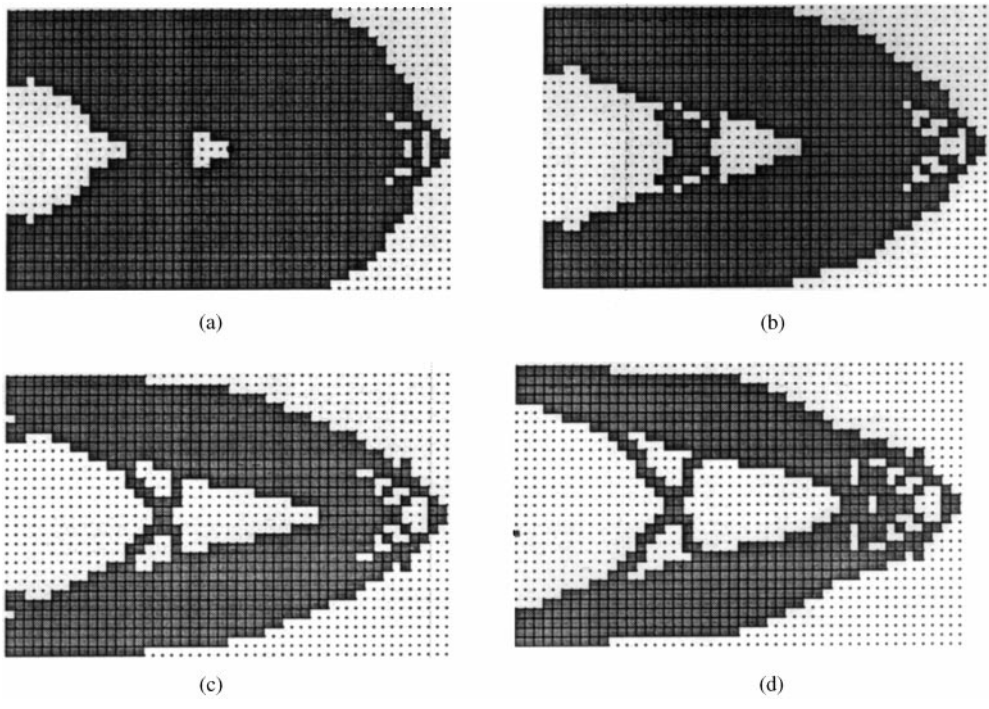

Figure 10. Optimization of the plane-stress plate model under symmetric load: (a) topology at iteration 27, weight ratio = 0·7875. $\sigma_A^2 = 0{\cdot}02357\ \text{mm}^2$; (b) topology at iteration 47, weight ratio = 0·6569. $\sigma_A^2 = 0{\cdot}02908\ \text{mm}^2$; (c) topology at iteration 70, weight ratio = 0·5458. $\sigma_A^2 = 0{\cdot}03963\ \text{mm}^2$; (d) optimum topology, weight ratio = 0·4556. $\sigma_A^2 = 0{\cdot}04971\ \text{mm}^2$.

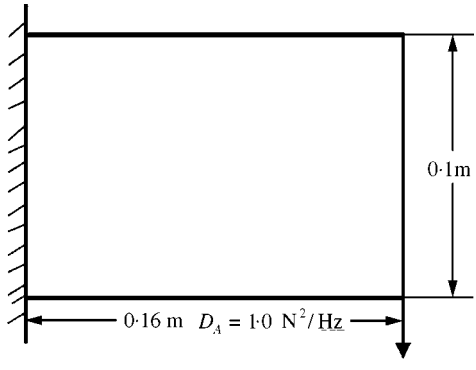

Figure 11. The initial structure model and loading case of a plane-stress plate under non-symmetric load.

preliminary result is that the effect of the truncated mode can be negligible if the mode is truncated in between two well-spaced frequencies. Also, the study in this paper only deals with distinct eigenvalue problems. Repeated or closed eigenvalues have been addressed in ESO for single natural frequency optimization [1] using a kind of average technique. It is expected that this technique can be equally used for response optimization as studied in this paper with reasonable accuracy. This topic is also under investigation at present.

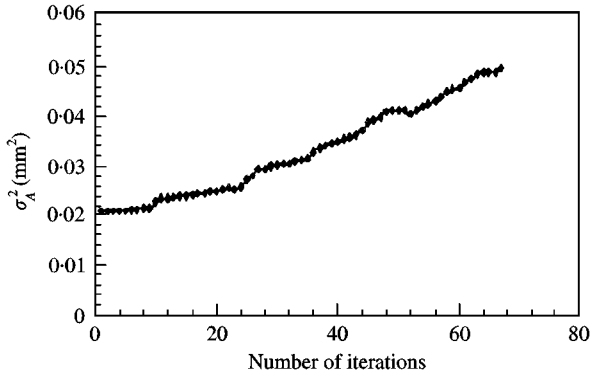

Figure 12. Evolutionary history of mean square dynamic responses at point *A*.

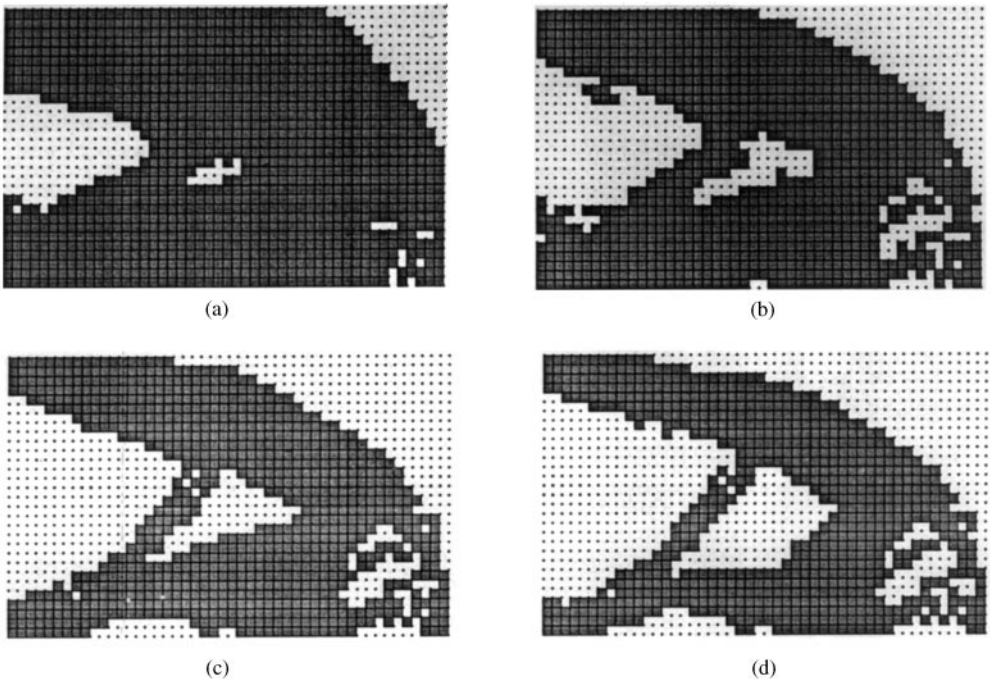

Figure 13. Optimization of the plane-stress plate model under non-symmetric load: (a) topology at iteration 16, weight ratio = 0·8375. $\sigma_A^2 = 0{\cdot}02094$ mm^2; (b) topology at iteration 34, weight ratio = 0·6875. $\sigma_A^2 = 0{\cdot}03122$ mm^2; (c) topology at iteration 51, weight ratio = 0·5771. $\sigma_A^2 = 0{\cdot}03998$ mm^2; (d) optimum topology, weight ratio = 0·4875. $\sigma_A^2 = 0{\cdot}04911$ mm^2.

5. CONCLUSION

The ESO method is applied for the optimization of mean square dynamic response. Aspects of the response description, sensitivity analysis and optimality criteria are presented. The ESO procedure is proposed and tested on optimization of plate structures. The results of topology and dynamic response demonstrate the validity and effectiveness of the proposed method.

REFERENCES

1. Y. M. XIE and G. P. STEVEN 1993 *Computers an Structures* **49**, 885–896. A simple evolutionary procedure for structural optimization.
2. Y. M. XIE and G. P. STEVEN 1996 *Computers and Structures* **58**, 1067–1073. Evolutionary structural optimization for dynamic problems.
3. Y. M. XIE and G. P. STEVEN 1997 *Evolutionary Structural Optimization*. Berlin: Springer.
4. N. OLHOFF 1974 *International Journal of Solids and Structures* **10**, 93–109. Optimal design of vibrating rectangular plate.
5. B. AKESSON and N. OLHOFF 1988 *Journal of Sound and Vibration* **120**, 457–463. Minimum stiffness of optimally located supports for maximum value of beam structures.
6. W. H. TONG and J. S. JIANG 1997 *Proceeding of* 3*rd Pacific International Conference On Aerospace Science and Technology*, *Xi'an*, *P.R. China*, 387–389. Some basic laws about dynamic optimization problems.
7. J. H. RONG 1996 *Mechanics Strength*, China **18**, 21–28. Dynamic response optimization of structures with damping.
8. R. GRANDHI 1993 *AIAA Journal* **31**, 2296–2303. Structural optimization with frequency constraints—a review.
9. M. P. BENDSØE and N. KIKUCHI 1988 *Computer Methods in Applied Mechanics and Engineering* **71**, 197–224. Generating optimal topologies in structural design using a homogenization method.
10. Z. D. MA, N. KIKUCHI and H. C. CHENG 1995 *Computer Methods in Applied Mechanics and Engineering* **121**, 259–280. Topology design for vibrating structures.
11. R. J. YANG and C. H. CHUANG 1994 *Computers and Structures* **52**, 265–275. Optimal topology design using linear programming.
12. R. J. YANG 1995 *American Society of Mechanical Engineers*, *Design Engineering Division* **124**, 393–398. Topology optimization analysis with multiple constraints.
13. A. R. MIJAR, C. C. SWAN, J. S. ARORA and I. KOSAKA 1998 *Journal of Structural Engineering*, *American Society of Civil Engineers* **124**, 541–550. Continuum topology optimization for concept design of frame bracing systems.
14. I. KOSAKA and C. C. SWAN 1999 *Computers and Structures* **70**, 47–61. A symmetry reduction methods for continuum structural topology optimization.
15. K. K. CHOI, E. F. HUAQNG and H. SEONG 1983 *International Journal for Numerical Methods in Engineering* **19**, 93–112. An iterative method for finite dimensional structural optimization problems with repeated eigenvalues.
16. R. L. DAILEY 1989 *AIAA Journal* **27**, 486–491. Eigenvectors derivatives with repeated eigenvalues.
17. S. H. CHEN and Z. S. LIU 1993 *Communications in Numerical Methods in Engineering* **9**, 427–438. Perturbation analysis of vibration modes with close frequencies.
18. D. T. SONG, W. Z. HAN and S. H. CHEN 1996 *AIAA Journal* **34**, 859–861. Simplified calculation eigenvector derivatives with repeated eigenvalues.
19. R. W. CLOUGH and J. PENZIEN 1993 *Dynamic of Structures*. Singapore: McGraw–Hill Book Co.
20. Z. S. LIU, S. H. CHEN and Y. Z. ZHAO 1994 *Computers and Structures* **52**, 1135–1143. An accurate method for computing eigenvector derivatives for free-free structure.
21. R. L. FOX and M. P. KAPOOR 1968 *AIAA Journal* **6**, 1067–1073. Rates of change of eigenvalues and eigenvectors.
22. W. C. MILLS-CURRAN 1988 *AIAA Journal* **26**, 861–871. Calculation of eigenvector derivatives for structures with repeated eigenvalues.
23. R. B. NELSON 1986 *AIAA Journal* **24**, 823–832. Simplified calculation of eigenvector derivatives.
24. I. U. OJALVO 1988 *AIAA Journal* **26**, 361–366. Efficient computation of modal sensitivities for systems with repeated frequencies.
25. B. P. WANG 1991 *AIAA Journal* **29**, 1018–1020. Improved approximate methods for computing eigenvector derivatives in structural dynamics.
26. R. T. HAFTKA and R.H. ADELMAN 1986 *AIAA Journal* **24**, 823–832. Sensitivity analysis of discrete structural systems.
27. J. F. BALDWIN and S. G. HUTTON 1985 *AIAA Journal* **23**, 1737–1743. Natural modes of modified structures.
28. D. N. CHU, Y. M. XIE, A. HIRA and G. P. STEVEN 1996 *Finite Elements in Analysis and Design* **21**, 239–251. Evolutionary topology optimization for problems with stiffness constraints.
29. Q. Q. LIANG, Y. M. XIE, G. P. STEVEN and L. C. SCHMIDT 1999 *Proceedings of the International Conference on Mechanics of Structures*, *Materials and Systems*, *Wollongong*, *Australia*, 309–315. Topology optimization of strut-and-tie model in non-flexural reinforced concrete members.